A&A 533, A115 (2011)
DOI: 10.1051/0004-6361/201117527

Astronomy & Astrophysics

Observations of the 2009 Leonid activity by the Tajikistan fireball network

G. I. Kokhirova[1] and J. Borovička[2]

[1] Institute of Astrophysics, Tajik Academy of Sciences, 734042 Dushanbe, Tajikistan
e-mail: Kokhirova2004@mail.ru
[2] Astronomical Institute of the Academy of Sciences of the Czech Republic, Ondřejov observatory, Fričova 298, 25165 Ondřejov, Czech Republic
e-mail: Jiri.Borovicka@asu.cas.cz

Received 20 June 2011 / Accepted 8 August 2011

ABSTRACT

The fireball network in Tajikistan operates since 2009. Observations of the 2009 Leonid activity were carried out on November 13−21. In this period 16 Leonid fireballs were photographed. As a result of astrometric and photometric reductions, the precise data including atmospheric trajectories, velocities, orbits, light curves, and photometric masses were determined for ten fireballs. Low-resolution video spectra were obtained for six fireballs.The radiant positions during the maximum night suggest that the majority of the fireball activity was caused by the annual stream component with only minor contribution of the 1466 trail. According to their end heights, nearly half of Leonid fireballs belonged to the most fragile and weak fireball group IIIB and the rest to the slightly more dense cometary group IIIA. However, one detected Leonid belonged to the fireball group I. This is the first detection of an anomalously strong Leonid individual. Its chemical composition was not markedly different from other Leonids.

Key words. meteorites, meteors, meteoroids

1. Introduction

The Leonids are a well-known meteor shower capable to produce meteor storms around November 17. The parent body is comet 55P/Tempel-Tuttle. Complex observations of the Leonids were performed both by ground-based and aircraft facilities during 1998−2002 and in 2006 in connection with the high activity of the shower at this period. Owing to extensive observational data, very important results were obtained, which significantly complemented meteor physics and dynamics and physical properties of cometary meteoroids. For the first time, extraordinary high beginning altitudes of the luminosity of the Leonid meteors were registered, among which some reach the limit of almost 200 km, and which are a result of both physical-chemical features of Leonid meteoroids and conditions of ablation at these altitudes (Spurný et al. 2000a,b; Koten et al. 2006).

According to several authors (Vaubaillon et al. 2005; Maslov 2007; Lyytinen & Nissinen 2009), high activity of the Leonids was predicted in 2009 as well.

We present here the results of the photographic observations of the 2009 Leonid meteor shower in Tajikistan. In Sect. 2 we describe the observations and data reduction. Then we provide the principal data on the fireball atmospheric trajectories (Sect. 3) and the analysis of the photographic beginning and end heights of fireball trajectories (Sect. 4). In Sect. 5 we give the coordinates of radiants and heliocentric orbits of the detected fireballs and a comparison of our data with the results of previous Leonid observations as well as with the forecasts for 2009. The light curves of fireballs, physical properties of the Leonid meteoroids and their spectral data are discussed in Sects. 6−8 respectively.

2. Observational data

The photographic observations of the Leonid activity in 2009 were carried out on November 13−21 by the fireball network, which consists of five stations situated on the southern part of the Tajikistan territory that cover an area of nearly eleven thousand square kilometers (Babadzhanov & Kokhirova 2009b). The distances between them range from 53 to 184 km. All stations of the network are equipped with fixed all-sky cameras with Zeiss Distagon "fish-eye" objectives (f = 30 mm, D/f = 1:3.5) using sheet films 9 × 12 cm, and with digital SLR cameras "Nikon D2X" and "Nikon D300" with the Nikkor "fish-eye" objectives (f = 10.5 mm, D/f = 1:2.8). To determine the time of the meteor appearance the guided camera mounted on the "Losmandy GM-8" equatorial mount in the Gissar astronomical observatory is used.

The symmetrical two-blade shutter rotates very closely to the focal plane of the cameras, yielding 10 or 12 breaks on the fireball trail per second. One digital camera is equipped with the shutter rotating in front of the objective and giving 15 breaks per second.

The exposure time for the fixed fireball cameras is usually four to eight hours, depending on the film sensitivity. The exposure time for the digital cameras is 30 s.

As a result of the observations, 16 Leonid fireballs were photographed, of which nine were registered on the night of maximum activity of November 17/18. Among all, three fireballs were photographed from five stations, one from four, two from three, seven from two, and three from one station.

Table 1. Data of the atmospheric trajectories of the fireballs.

ID number	131109	171109*A*	171109*B*	171109*C*	171109*D*	171109*E*	171109*F*	171109*G*	191109	211109
Date, 2009	Nov. 13	Nov. 17	Nov. 17	Nov. 17	Nov. 17	Nov. 17	Nov. 17	Nov. 17	Nov. 19	Nov. 21
Time (UT)	22:09:01	20:39:09	20:49:56	21:10:25	21:24:05	22:17:14	22:37:37	23:35:27	22:14:41	21:47:39
$L_\odot^\circ$	231.535	235.504	235.511	235.526	235.535	235.572	235.590	235.627	237.589	239.590
v (km s^{-1})	71.80	71.84	72.07	71.45	71.77	71.71	71.59	70.57	70.38	71.78
	±.16	±.05	±.17	±.38	±.18	±.60	±.53	±.49	±.36	±.03
h_B (km)	108.50	111.21	112.38	107.66	114.56	114.06	106.45	106.68	104.26	110.33
	±.04	±.01	±.02	±.09	±.02	±.01	±.29	±.01	±.01	±.02
h_E (km)	91.14	91.03	91.51	91.05	98.91	77.84	89.04	87.01	91.05	98.20
	±.03	±.00	±.04	±.07	±.02	±.01	±.28	±.01	±.02	±.01
l (km)	26.4	51.2	50.3	32.9	29.9	55.1	24.7	23.8	19.9	21.2
$M_{\max}$	−8.0	−7.2	−8.5	−6.6	−3.7	−3.4	−9.1	−6.4	−6.3	−7.5
m_∞ (kg)	.008	.007	.019	.004	.0002	.00025	.017	.002	.002	.004
P_E	−5.82	−5.64	−5.90	−5.69	−5.76	−4.40	−5.98	−5.51	−5.67	−6.34
Type	IIIB	IIIA	IIIB	IIIA	IIIB	I	IIIB	IIIA	IIIA	IIIB

The time of the fireball appearance was determined either by combining the fireball images obtained by the fixed and guided cameras, or by the digital fireball image. During the maximum night, double station and spectral video observations were performed simultaneously (Koten et al. 2011). For the six fireballs reported here, spectra were captured by the video camera. We were able to extract more precise times of the fireball appearance from the video tapes. Here we present precise data only of the ten photographed fireballs for which the coordinates of radiants, heights, velocities, light curves, and orbital elements were determined. The geometrical conditions for the other three double-station fireballs were insufficient to compute reliable trajectories. The fireball photographs were measured using the Zeiss Ascorecord x, y measuring maschine. Digital fireball images were measured on the PC with our own software "FISHSCAN".

The astrometric reduction procedures are the same as in the European Fireball Network, which allow one determine the position of an object at any point of photographic frame with the precision of one arc minute or better (Borovička et al. 1995; Babadzhanov et al. 2009).

3. Atmospheric trajectories

The basic parameters of atmospheric trajectories of fireballs are given in Table 1, which contains the following data: the ID number of the fireball according to its date of occurrence and denoted *ddmmyy* where *dd* is the day, *mm* is the month and *yy* are the last two digits of the year. This way fireballs of the same day are distinguished by adding a capital letter after the notation; date, the time of the fireball passage in UT; $L_\odot$ is the longitude of the Sun corresponding to the time of the fireball passage (J2000.0); v is the fireball velocity; h_B and h_E are the beginning and the terminal heights of the luminous trajectory above the sea level; l is the total length of the luminous trajectory; M_P is the maximum absolute magnitude of the fireball; m_∞ is the initial photometric mass of the meteoroid; P_E is empirical end height criterion for fireballs; the type of fireball according to Ceplecha & McCrosky (1976) classification. The standard deviations given for the beginning and the terminal points reflect the precision in computing the heights and positions of fireballs in the atmosphere.

Note that for all fireballs it was impossible to determine the decelerations along the trajectories reliably. The cameras are not particularly suitable for studying velocities of very fast meteors like Leonids, because the shutter frequency is relatively low (12−15 breaks per second). In some cases we had to rely on three or four shutter breaks. Therefore, only average velocities were computed and were assumed to be equal to the initial velocities.

4. Photographic beginning and end heights of visible fireball trajectories

It is undoubted now that the limit of beginning heights of bright high-velocity meteors reaches 200 km.

This was confirmed by observations of the Leonids storm and outbursts during 1998−2002. The techniques used then are more sensitive than the photographic techniques and provided a large number of meteors registered at beginning heights between 130−200 km (see, e.g., Spurný et al. 2000a,b; Koten et al. 2006).

Our observational equipment does not allows us to record meteors at such heights because for the film's sensitivity I = 125 ISO units the limiting magnitudes of registration of meteors is equal to about −4 mag, while, as was shown by Spurný et al. (2000a) and Koten et al. (2006), a brightness of meteors at heights above 130 km is more than 0 mag, as a rule.

The range of beginning heights of the fireballs under investigation photographed by the all-sky cameras was between 114−104 km. The beginning heights registered by the digital camera were between 128−114 km. This difference is caused by the greater sensitivity of the digital camera. The standard range of terminal heights was 98−87 km for the all-sky cameras and practically the same for the digital ones. The reason is that the decrease of brightness at the end of the fireballs was very steep. One case of terminal height of 77.8 km was fixed only by the digital camera.

From the all-sky photographic records of Leonid fireballs Shrbený & Spurný (2009) obtained the value 111 ± 5 km for the beginning height for the range of maximum absolute magnitudes from −3 to −14, and concluded that this is the limiting altitude of all Leonids for the registration by the all-sky cameras. Our data agree with their conclusion.

Spurný et al. (2000b) investigated photographic and TV heights of high-altitude Leonid meteors (h_B > 116 km) and found that the photographic beginning height of a meteoroid weakly depends on its initial mass or maximum absolute magnitude. But the authors revealed a relatively strong correlation on the end heights, which is that very bright Leonid meteors, that consequently have greater mass, penetrate more than 20 km deeper than the faintest ones. Our sample does not cover such a wide range of meteoroid masses, and we see only a slight tendency of decreasing end height with mass.

However, the fireball TN171109*E* with the maximal magnitude −3.4 and initial mass of only 2.5×10^{-4} kg was quite anomalous in this respect because it penetrated to the terminal height of 77.8 km, much deeper than more massive bodies.

5. Radiants and heliocentric orbits of fireballs

Table 2 gives the results of the determination of the coordinates of radiants and heliocentric orbits of the Leonid fireballs with their standard deviations. Here α_R, δ_R are the right ascension and declination of the apparent radiant of fireball at the time of observation; z_R is the zenith distance of the apparent radiant; Q_p is the convergence angle between two planes (for multi-station fireballs the widest angle from all combinations of planes); v_∞ is the initial (preatmospheric) velocity; α_g, δ_g are the right ascension and declination of the geocentric radiant of fireball in J2000.0 equinox; v_g is the geocentric velocity; v_h is the heliocentric velocity; $a, e, q, \omega, \Omega, i$ are the orbital elements in J2000.0 equinox. The results of determination of the coordinates of radiants of Leonid fireballs photographed during November 13–21, 2009, depending on the longitude of the Sun, are illustrated in Fig. 1 and compared with previously published radiant drifts. Using only our data, the daily radiant drift was found to be $\Delta\alpha = 0.78°$ and $\Delta\delta = -0.53°$. Maximum activity of Leonids occurred on the night of November 17/18 at the solar longitude near 235.56°, which corresponds to the time 22:07 UT (Koten et al. 2011). The enhanced activity was predicted to be produced by two meteoroid trails ejected from the parent comet in 1466 and 1533, and peaking roughly at the same time of November 17/18 2009, 21:43 and 21:50 UT, respectively (Vaubaillon et al. 2009). The annual Leonid shower was expected to peak approximately at the same time but with much lower activity. Figure 2 shows the radiant positions of Leonids observed that night together with the predicted radiants for the 1466 and 1533 trails (Vaubaillon et al. 2009), the radiant of the annual shower according to various authors, and the so-called filament circle along which the radiants were spread during 2006 Leonids (Jenniskens et al. 2008). The error of the radiants of two Leonids (*D* and *F*) is too large to judge their origin. The radiant *C*, with moderate error, lies in between the annual radiant and the 1466 trail. The quite precise radiants *A*, *B*, and *G* lie closer to the annual shower or to the filament circle. Radiant *E* is the only one that can be attributed with some confidence to the 1466 trail, because it lies much closer to the predicted radiant of the 1466 trail than to the radiants of annual Leonids and because its error is small. None of the seven fireballs can be firmly attributed to the 1533 trail. Note that the time of the fireball occurrence does not allow to distinguish between the annual component and the trails.

The mean geocentric radiant of Leonid fireballs on November 17/18, 2009, is $\alpha = 153.66° \pm 0.17°$ and $\delta = 22.11° \pm 0.31°$ for $L_\odot = 235.5°$, and is very close to the mean radiant values of Leonid fireballs in 1998 $\alpha = 153.63°$, $\delta = 22.04°$ for $L_\odot = 235.1°$ (Betlem et al. 1999) and in 1999–2006 $\alpha = 153.6° \pm 0.4°$, $\delta = 22.0° \pm 0.4°$ for $L_\odot = 235.1°$ (Shrbený & Spurný 2009).

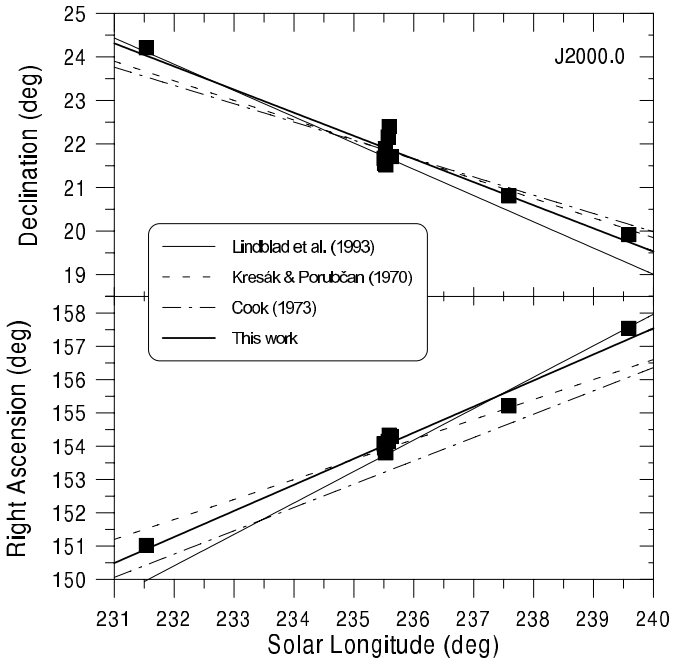

Fig. 1. Drift of Leonid radiant as a function of solar longitude. Our observations (black squares) are compared with three published drifts as quoted in Jenniskens (Jenniskens 2006). A linear fit to our data is also shown. All coordinates are given in the equinox J2000.0.

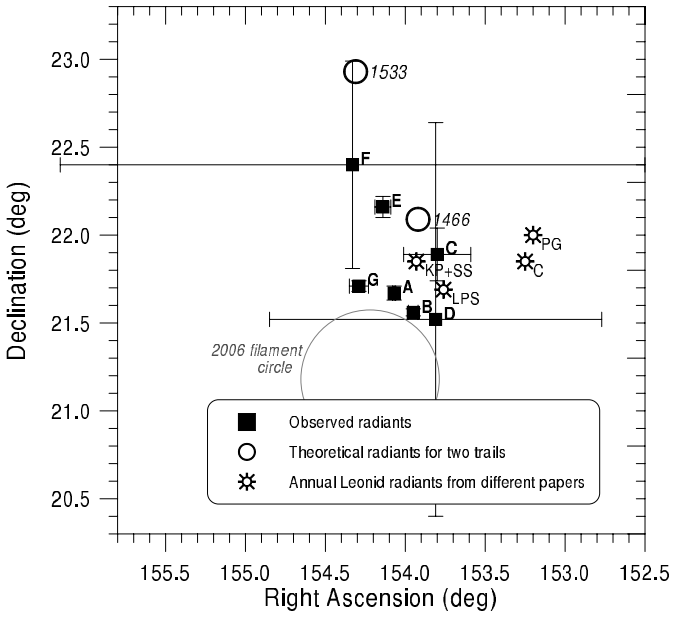

Fig. 2. Leonid radiants during the maximum on November 17, 2009. The observed radiants are shown with their errors and compared with theoretical radiants for the 1466 and 1533 trails (Vaubaillon et al. 2009), with the annual Leonid radiant at solar longitude 235.55° according to Cook (1973) (C), Kresák & Porubčan (1970) (KP), Lindblad et al. (1993) (LPS), Porubčan & Gavajdová (1994) (PG), and Shrbený & Spurný (2009) (SS, radiant almost identical to KP). The filament circle as observed in 2006 (Jenniskens et al. 2008) is also shown. All coordinates are given in the equinox J2000.0.

6. Light curves of fireballs

The photometry of Leonid fireballs was performed by the method developed for photographs taken by the Czech fish-eye camera (Ceplecha 1987). This method allows one determine a brightness of the fireball with the photometric precision of ±0.2 stellar magnitudes in the whole field to a zenith distance to 70°. Negatives, where fireball images have the best quality

Table 2. Coordinates of radiants and heliocentric orbits of the fireballs.

ID number	131109	171109*A*	171109*B*	171109*C*	171109*D*	171109*E*	171109*F*	171109*G*	191109	211109
α_R°	151.04	153.87	153.77	153.70	153.73	154.17	154.42	154.51	155.26	157.51
	±.09	±.04	±.02	±.14	±1.11	±.01	±.58	±.03	±.07	±.07
δ_R°	24.23	21.76	21.65	21.96	21.58	22.18	22.44	21.73	20.85	19.99
	±.07	±.01	±.03	±.21	±1.03	±.01	±1.81	±.06	±.03	±.02
$\cos z_R$	.658	.390	.412	.503	.523	.655	.705	.828	.663	.572
Q_p°	51	74	55	25	5	33	17	74	62	58
α_g°	151.02	154.07	153.95	153.81	153.81	154.14	154.33	154.29	155.21	157.54
	±.09	±.04	±.02	±.15	±1.12	±.02	±.59	±.03	±.07	±.07
δ_g°	24.21	21.66	21.56	21.89	21.52	22.16	22.40	21.71	20.81	19.92
	±.08	±.01	±.03	±.21	±1.04	±.01	±1.83	±.06	±.03	±.02
v_∞ (km s^{-1})	71.80	71.84	72.07	71.45	71.77	71.71	71.59	70.57	70.38	71.78
	±.16	±.05	±.17	±.38	±.18	±.60	±.53	±.49	±.36	±.03
v_g (km s^{-1})	70.66	70.64	70.87	70.26	70.59	70.56	70.47	69.50	69.22	70.61
	±.16	±.05	±.17	±.38	±.18	±.60	±.54	±.50	±.37	±.04
v_h (km s^{-1})	41.64	41.35	41.56	40.99	41.26	41.34	41.31	40.24	39.85	41.23
	±.16	±.05	±.17	±.38	±.25	±.60	±.60	±.50	±.36	±.04
a (AU)	14.91	10.44	13.15	7.73	9.61	10.40	10.05	5.05	4.28	9.21
	±3.38	±.49	±2.80	±2.11	±2.12	±6.04	±5.66	±1.15	±0.60	±0.28
e	.934	.906	.925	.873	.897	.905	.902	.805	.770	.893
	±.015	±.004	±.016	±.035	±.023	±.055	±.055	±.044	±.032	±.003
q (AU)	.983	.984	.984	.985	.985	.985	.984	.983	.986	.984
	±.000	±.000	±.000	±.001	±.004	±.000	±.003	±.000	±.000	±.000
ω°	170.80	171.78	172.13	172.81	172.46	172.48	172.26	170.94	173.85	172.98
	±.30	±.13	±.11	±.58	±3.78	±.30	±3.19	±.35	±.29	±.21
Ω°	231.53	235.50	235.51	235.53	235.53	235.57	235.59	235.63	237.59	239.59
	±.00	±.00	±.00	±.00	±.00	±.00	±00	±.00	±.00	±.00
i°	160.04	162.35	162.63	162.09	162.72	161.53	161.01	161.94	162.80	163.07
	±.13	±.03	±.06	±.35	±1.77	±.11	±2.89	±.14	±.09	±.06

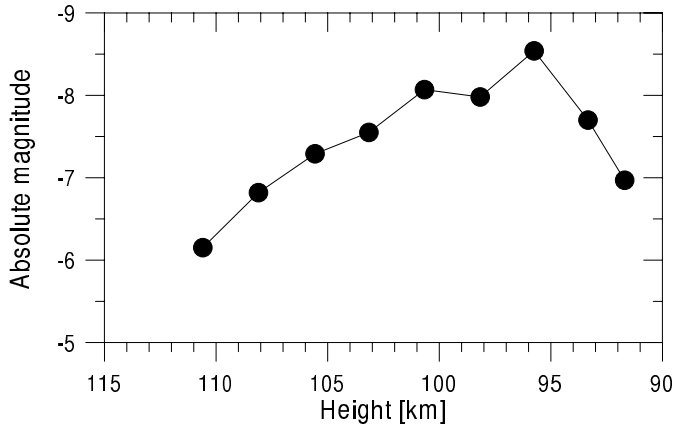

Fig. 3. Observed light curve of Leonid fireball TN171109*B*.

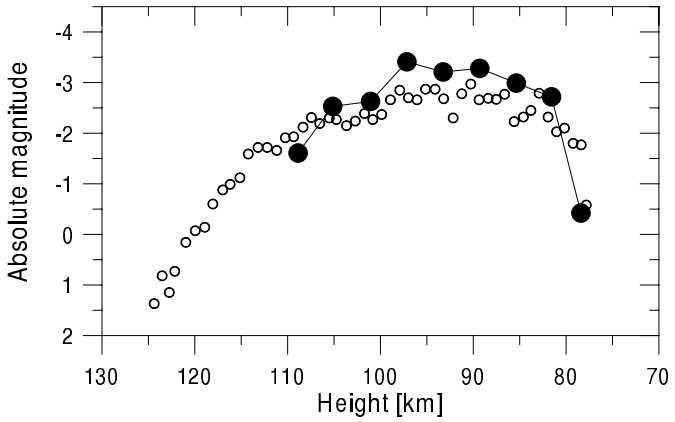

Fig. 4. Observed light curve of Leonid fireball TN171109*E*. The empty circles are approximate magnitudes from the spectral video camera.

and a greater number of breaks, were used for photometry. The photometry of two fireballs observed only by the digital cameras was performed with the "FISHSCAN" program.

Maximum absolute magnitudes and initial photometric masses are given in Table 1. The maximum absolute magnitude ranges between −3.4 and −9.1, the masses are between 0.2 and 20 grams. The typical observed light curve of the fireball TN171109*B* is presented in Fig. 3. We also present the light curve of the deeply penetrating fireball TN171109*E* in Fig. 4. All registered fireballs except TN171109*F* have smooth light curves with no significant flares. Almost all curves have an asymmetric shape and the maximum points shifted toward to the end of luminosity.

7. Physical properties of Leonid meteoroids

The values of the empirical P_E criterion given in Table 1 and calculated by the following expression (Ceplecha & McCrosky 1976):

$$P_E = \log \rho_E - 0.42 \log m_\infty + 1.49 \log v_\infty - 1.29 \log \cos z_R,$$

where ρ_E – is the air density (g cm^{-3}) at the h_E – the terminal height of the fireball visible trajectory (US Standard Atmosphere 1962), indicate the penetration ability of a meteoroid; m_∞ is given in grams and v_∞ in km s^{-1}. For majority of fireballs the P_E values are typical for the fireballs of types IIIA and IIIB according to Ceplecha & McCrosky (1976) classification. The fireballs of group IIIA are characterized by the mean bulk density of $\delta = 0.6$ g cm^{-3} while the fireballs of group IIIB are produced by

Table 3. List of recorded fireball spectra.

Fireball	Spectrum	Order	Note
TN171109*B*	SX1124	0	below 101 km
		−1	saturated
		−2	to 670 nm
TN171109*C*	SX1127	−2	
TN171109*D*	SX1129	−1	from 500 nm
		−2	too faint
TN171109*E*	SX1139	+1	tiny part
		0	
		−1	
TN171109*F*	SX1144	−1	saturated
		−2	
TN171109*G*	SX1157	−1	saturated
		−2	to 790 nm

the meteoroids with the lowest bulk density that is estimated to about $\delta = 0.2$ g cm^{-3}, and represent the weakest cometary material. The fireball TN171109*E* was classified as type I, which is an absolute exception among Leonids and quite unusual for fireballs on cometary orbits. Type I fireballs are normally associated with stony meteoroids with a density of about 3.5 g cm^{-3}. The existence of different fireball types among the Leonid fireballs was, however, also noted by Shrbený & Spurný (2009). They recognized fireballs corresponding to types II, IIIA, and IIIB according to the P_E criterion and made a conclusion on non-homogeneity of the parent comet.

On the base of photographic observations of Leonids Babadzhanov & Kokhirova (2009a) determined the mean bulk density to be equal to $\delta = 0.4 \pm 0.1$ g cm^{-3}, and the mean mineralogical density of $\delta_m = 2.3 \pm 0.2$ g cm^{-3} of these meteoroids. Using the relation between these densities, the porosity of Leonid meteoroids was calculated to be $p = 83\%$. These confirm the very porous and fragile structure of the Leonid meteoroids. It turned out that the density and porosity of Leonid meteoroids are very similar to those of Draconid meteoroids, which were also found to be porous aggregates of the constituent grains with a bulk density of $\delta = 0.3$ g cm^{-3} and porosity of $p = 90\%$ (Borovička et al. 2007).

The range of values of the mean bulk density $\delta = 0.6–0.2$ g cm^{-3} of the Leonid meteoroids under investigation obtained according to the calculated values of P_E criterion and fireball types agrees well with the mentioned results of the investigation of density and porosity of cometary meteoroids. The nature of TN171109*E* with a likely much higher bulk density is puzzling in this context. Nevertheless, small strong constituents penetrating much deeper than the majority of the meteoroid were observed in Leonids before (Spurný et al. 2000a; Borovička & Jenniskens 2000). TN171109*E* is the first case where a whole Leonid meteoroid was so strong that it was classified as a type I meteoroid.

8. Spectra

Spectra of six fireballs were captured by the spectral video camera operated at the Kurgan Tube station during the maximum night. The camera – an analog camcorder Panasonic NV-S88E equipped with a second-generation image intensifier Mullard XX1332, the lens 1.4/50 mm, and a 600 grooves/mm blazed transmission grating in front of the lens – was part of a double station video experiment of Koten et al. (2011). Data were recorded continuously on S-VHS tapes. The camera had a circular field-of-view with diameter of 55° and was aimed 50° above the NNW horizon. Spectra of meteors appearing on the NW, where the non-spectral camera was aiming, were captured in the +1st first order. Sufficiently bright fireballs appearing on N or NNE were captured in the −1st first or −2nd second order (i.e. on the non-blazed side of the grating). Because the camera was sensitive and had a resolution of only 8 bit per pixel, spectra of bright fireballs were saturated in the −1st first order. Table 3 gives the list of recorded fireball spectra. The order zero means direct imaging of the fireball. None of the fireballs was captured by the non-spectral video cameras, except for a very small part of fireball TN171109*E*.

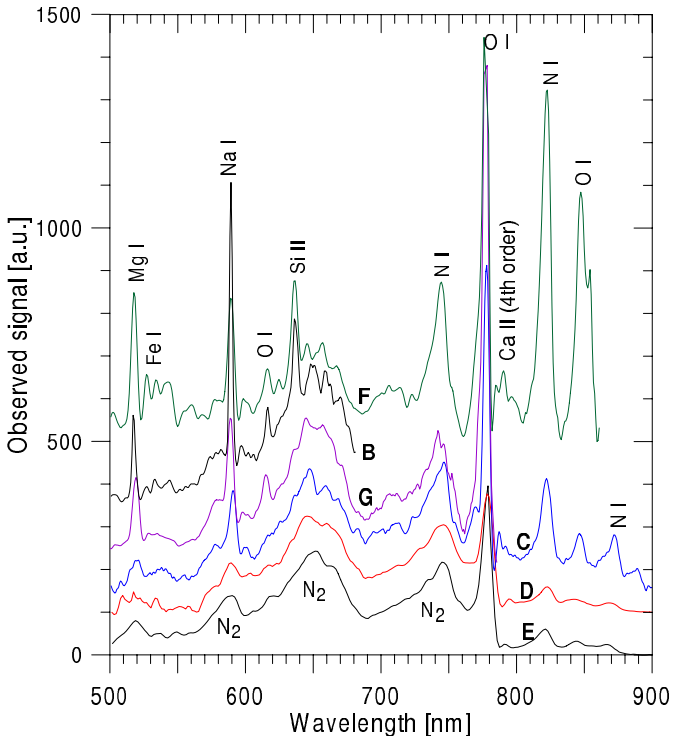

Fig. 5. Raw spectra of fireballs TN171109*B* to TN171109*G* at their maximum light. The observed signal is plotted as a function of wavelength. Fireballs *D* and *E* were captured in the −1st first spectral order and their spectra have therefore half the resolution of the spectra of all other fireballs, which were captured in the −2nd second order. Because the camera sensitivity as a function of wavelength differs in different orders, the observed signal of fireballs *D* and *E* was recomputed as if they were observed in the −2nd second order. For clarity the spectra have been offset vertically. Fainter spectra are given at the bottom, the brightest spectrum (fireball *F*) is at the top. The top of the brightest line, O I at 777 nm, was cut in spectra *G* and *F*.

The spectra are shown in Fig. 5. Most of the spectra could be studied from 500 to 850 nm. In some cases the wavelength range was shorter but the most important lines were seen in all spectra. The appearance of the spectra is the same as for the 1998 Leonids studied by Borovička et al. (1999). There is a continuum, N_2 molecular bands, O and N lines of atmospheric origin, and Mg, Na, and Fe lines from meteoric vapors. The importance of meteoric lines relative to N_2 bands increased with meteor brightness. Moreover, in the brightest observed fireballs, the high-temperature meteoric component represented here by the lines of ionized Si and ionized Ca was also present.

In Fig. 6 monochromatic light curves in the Mg and Na lines can be compared. The Na line was relatively fainter (compared to Mg) in fainter meteors, a trend also seen in 1998 Leonids. Another effect important in 1998 Leonids was the preferential

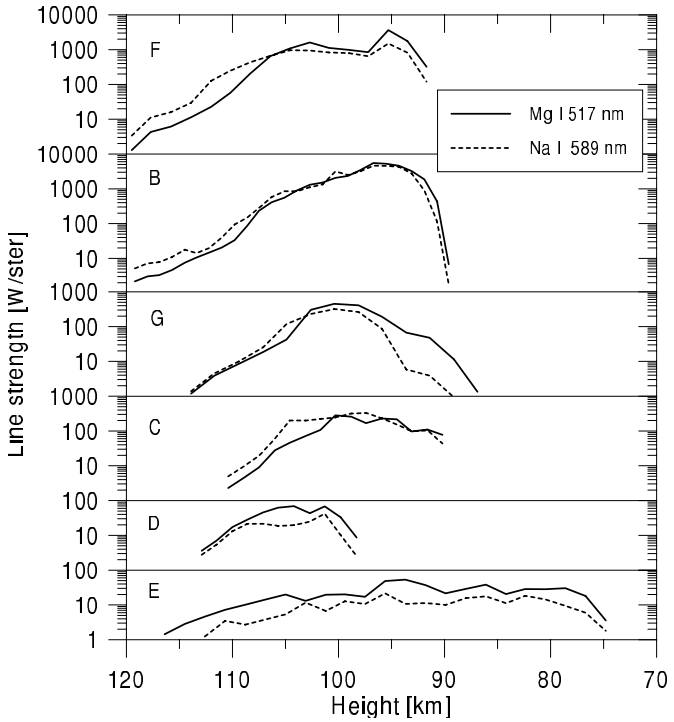

Fig. 6. Strength of Mg I (solid curves) and Na I (dashed curves) lines as a function of height in the spectra of fireballs TN171109*B* to TN171109*G*. Fainter fireballs are given at *the bottom*.

ablation of Na in the upper part of the trajectories. The effect was most pronounced in faint meteors but also in bright meteors the Na/Mg ratio decreased along the trajectory. We can see that this was also the case in the 2009 Leonid fireballs, except for TN171109*E*, where the Na/Mg ratio was nearly constant (and fairly low).

We interpret the preferential ablation of Na as a demonstration of differential ablation. In very small meteoroids, Na and K are able to evaporate from the whole volume at the beginning of ablation, earlier than other elements (Janches et al. 2009). It follows that in large meteoroids the Na line can be shifted to higher altitudes if the meteoroid is disintegrating into small grains. That was evidently not the case for the anomalously strong TN171109*E*. There is no other spectral evidence of any exotic nature of TN171109*E*. The Na content was fairly low but not different from TN171109*D*.

9. Conclusions

As a result of photographic observations by the Tajikistan fireball network during November 13–21, 2009, 16 Leonid fireballs were registered, of which nine fireballs were captured on the night of the maximum on November 17/18. This number confirms the forecasted enhanced activity of Leonids in 2009. The results of the determination of the precise atmospheric trajectories, velocities, initial masses and orbits of ten Leonid fireballs were presented in this study. For six fireballs low-resolution spectra were obtained as well.

The daily radiant drift of Leonids was found to be $\Delta\alpha = 0.78°$ and $\Delta\delta = -0.53°$. The radiant positions during the maximum night suggest that the majority of the fireball activity (i.e. the majority of flux of Leonid meteoroids higher than 0.2 g) was caused by an annual stream component with only minor contribution of the 1466 trail. This is not surprising because the trails were not expected to be rich in bright meteors.

According to the P_E criterion, almost all Leonid fireballs belonged to the fireball groups IIIA and IIIB that have a cometary origin, and correspond to the meteoroid mean bulk density of about 0.6 and 0.2 g cm^{-3} and porosity of 80–90%. However, one detected Leonid with a size of about 5 mm belonged to the fireball group I and likely had a bulk density of few g cm^{-3}. This is the first detection of an anomalously strong Leonid individual. Its chemical composition was not markedly different from other Leonids.

Acknowledgements. The authors would like to express gratitude to specialists of the Institute of Astrophysics of Tajik Academy of Sciences M. I. Gulyamov, A. Sh. Mullo-Abdolov, A. O. Yulchiev, U. Kh. Khamroev, S. P. Litvinov, and to Dr. P. Koten (Astronomical Institute of the Academy of Sciences of the Czech Republic), who participated in the observations and data reduction, and to Dr. J. Vaubaillon for useful comments which improved the paper. The annotations by the A&A Language Editor A. Peter are also appreciated. This work was supported by the International Science and Technology Centre Project T-1629. Spectral analysis was supported by GAČR grant No. P209/11/1382.

References

Babadzhanov, P. B., & Kokhirova, G. I. 2009a, A&A, 495, 353
Babadzhanov, P. B., & Kokhirova, G. I. 2009b, Izv. Akad. Nauk Resp. Taj., 2(135), 46
Babadzhanov, P. B., Kokhirova, G. I., Borovička, J., & Spurný, P. 2009, Sol. Syst. Res., 43, 353
Betlem, H., Jenniskens, P., Van't Leven, J., et al. 1999, Meteorit. Plan. Sci., 34, 979
Borovička, J., & Jenniskens, P. 2000, Earth, Moon and Planets, 82, 399
Borovička, J., Spurný, P., & Keclíková, J. 1995, A&AS, 112, 173
Borovička, J., Štork, R., & Boček, J. 1999, Meteorit. Plan. Sci., 34, 987
Borovička, J., Spurný, P., & Koten, P. 2007, A&A, 473, 661
Ceplecha, Z. 1987, Bull. Astron. Inst. Czechosl., 38, 222
Ceplecha, Z., & McCrosky, R. E. 1976, J. Geophys. Res., 81, 6257
Cook, A. F. 1973, in Evolutionary and Physical Properties of Meteoroids, ed. C. L. Hemenway, P. M. Millman, & A. F. Cook, NASA SP-319, Washington, DC, 183
Janches, D., Dyrud, L. P., Broadley, S. L., & Plane, J. M. C. 2009, Geophys. Res. Lett., 36, L06101
Jenniskens, P. 2006, Meteor Showers and their Parent Comets (New York: Cambridge Univ. Press), 790
Jenniskens, P., de Kleer, K., Vaubaillon, J., et al. 2008, Icarus, 196, 171
Koten, P., Spurný, P., Borovička, J., et al. 2006, Meteorit. Plan. Sci., 41, 1305
Koten, P., Borovička, J., & Kokhirova, G. I. 2011, A&A, 528, A94
Kresák, L., & Porubčan, V. 1970, Bull. Astron. Inst. Czechosl., 21, 153
Lindblad, B. A., Porubčan, V., & Štohl, J. 1993, In Meteoroids and their Parent Bodies, ed. J. Štohl, & I. P. Williams, Slovak Acad. Sci., Bratislava, 177
Lyytinen, E., & Nissinen, M. 2009, WGN, 37, 122
Maslov, M. 2007, WGN, 35, 5
Porubčan, V., & Gavajdová, M. 1994, Plan. Space Sci., 42, 151
Shrbený, L., & Spurný, P. 2009, A&A, 506, 1445
Spurný, P., Betlem, H., Jobse, K., Koten, P., & Van't Leven, J. 2000a, Meteorit. Plan. Sci., 35, 1109
Spurný, P., Betlem, H., Van't Leven, J., & Jenniskens, P. 2000b, Meteorit. Plan. Sci., 35, 243
Vaubaillon, J., Colas, F., & Jorda, L. 2005, A&A, 439, 761
Vaubaillon, J., Atreya, P., Jenniskens, P., et al. 2009, November 16, Central Bureau Electronic Telegram, 2019
US Standard Atmosphere 1962 (Washington, D.C.: US Government Printing Office 1963), 278